This article has been accepted for publication in a future issue of this journal, but has not been fully edited. Content may change prior to final publication. Citation information: DOI 10.1109/LAWP.2021.3115234, IEEE Antennas and Wireless Propagation Letters

Low-Profile CPW-PS Fed Magneto-Electric Antenna

Aditya Singh and Carlos E. Saavedra

***Abstract*—A magneto-electric antenna (MEA) that uses coplanar waveguide (CPW) to parallel strip (PS) line transition as feed to obtain a wide bandwidth is presented for millimeter wave bands. The balanced feed is utilized to feed a modified ME-dipole. The modified structure consists of a simple two metal strips ME antenna loaded with metallic loops. The resonant modes study shows that a new resonant mode is contributed by the loop when the loop length is nearly a wavelength thereby improving the impedance bandwidth (IBW) and realized gain. A prototype is fabricated in-house with printed circuit board (PCB) technology. Measured results validate fractional IBW (VSWR $\leq$ 2) of 75.76% with realized gain being 8.6$\pm$1.8 dBi for 14 to 29 GHz. The radiation pattern measurements indicate stable radiation pattern across the band with low broadside cross-polarization levels in both E and H planes. The simulated total efficiency is 86-96%.**

***Index Terms*—millimeter wave, antenna, magneto-electric dipole, CPW-PS line, balanced feed, loop, wideband, Ku-band, K-band, Ka Band.**

I. Introduction

MILLIMETER-WAVE (mm-wave) antennas with wide impedance bandwidth are desired for fifth generation communications system (5G mm-wave). Magneto-electric (ME) dipole antennas are well suited to deliver high gain and wide impedance bandwidth (IBW) requirements in the mm-wave band. These antennas proposed first in [1] exploit equally excited magnetic and electric dipoles to provide wide IBW and identical patterns in the E and H planes. To feed these antennas, various methods have been employed including Γ-shaped [2] and L-shaped probes [3], direct coaxial line feed [4], microstripline (MSL) to aperture [5], MSL to L-shaped probe [6], [7], substrate integrated waveguide (SIW) to aperture [8], among others. These methods provide good IBW, gain and polarization characteristics for the antenna. However, many use intricate shapes for the probes and need metallic vias. Moreover, simple probe feeds are difficult to be interfaced with other circuits and unbalanced feeds may limit the achievable IBW.

Numerous works have reported ME antennas in the mm-wave bands [5]–[7], [9]–[12]. In [5], an aperture-coupled simple MEA is proposed. It uses 2 different substrates to house a microstrip line to feed the aperture slot. Two metal strips with a small gap are used as ME dipole in the mm-wave band to obtain 29.1% IBW (VSWR $\leq$ 2) with simulated gain of 8.3$\pm$0.7 dBi with an antenna profile of 0.165λ_0 where λ_0 is the free space wavelength at the center frequency. Furthermore, authors in [7], propose antenna element feed that uses packaged MSL to L-probe transition in multilayered printed circuit board (PCB). The element itself utilizes four shorted patches using metallic vias to obtain ME operation. Three resonances are observed with fractional IBW ($|S_{11}| \leq$ -10 dB) of 54.4% at 32.15 GHz with average gain of 7.35 dBi while the back lobe is reduced due to packaged MSL. In [9], the antenna element uses a pair of printed dipoles and small shorted patch on a multilayered PCB. A microstripline housed in a thin hybrid substrate feeds a wide slot whereby exciting the top ME structures. The antenna shows 3 resonant modes to obtain an IBW ($|S_{11}| \leq$ -10 dB) of 42.8% and maximum gain of $\sim$9 dBi with good gain flatness. The total profile of the antenna is 0.168λ_0. To further enhance the IBW, differential feed systems can be used. For example, [10] presents an ultrawideband (UWB) design where 2 SMA connectors are used. A vertical MSL to PS line transition is used to feed shorted patches. The profile of antenna is $\sim$0.29λ_0 while the overall size is $\sim$2.2λ_0^2. However, the design is aimed for 3.1 - 10.6 GHz band and utilizes a metallic cavity to reduce the back lobes and improve the broadside gain.

In this letter, a wide-band loop-loaded MEA employing a balanced CPW-PS line feed with a single feed port is proposed. The CPW-PS transition is used to feed a simple MEA to show the improvement in IBW of a simple ME radiator. Further modification is proposed to achieve a wider IBW by loading the simple MEA with a metallic loop. The excitation of new resonant mode contributed by near wavelength long resonant loop also enhances the realized gain while maintaining a simple antenna structure.

II. Antenna Design

A. Feeding Mechanism

Fig.1 (a) shows the exploded view of the proposed antenna. The antenna feed system consists of a 50 Ω coplanar waveguide (CPW) designed on a 0.5 mm thick Rogers-4003 substrate (ϵ_r = 3.55, $\tan\delta$ = 0.0027). The width of the signal trace of the CPW is w_c and truncated near the feeding end so that an end-launch 50 Ω connector [13] can be used as shown in Fig.1 (a). The conductivity of the connector alloy is considered to be same as copper. The CPW line is terminated in an open circuit with slot width as s_{cps} and a transition to parallel-strip (PS) line is introduced at the open end. The PS line is designed on 0.5 mm thick Rogers-5880 substrate (ϵ_r = 2.2, $\tan\delta$ = 0.0009) of width w_c with copper layers of thickness t on both the sides as shown in Fig.1 (b). The two metal strips connect to CPW signal trace and ground plane to provide wideband unbalanced CPW line to balanced PS feed line [14] for the ME dipole antenna. All the design parameters are tabulated in Fig.1.

Submitted September 22, 2021. This work was supported, in part, by the Natural Sciences and Engineering Research Council of Canada (NSERC) Strategic Project under Grant STPGP-521223-2018.

The authors are with the Department of Electrical and Computer Engineering, Queen's University, Kingston, Ontario, Canada, K7L 3N6. (e-mail: singh.aditya@queensu.ca)

This article has been accepted for publication in a future issue of this journal, but has not been fully edited. Content may change prior to final publication. Citation information: DOI 10.1109/LAWP.2021.3115234, IEEE Antennas and Wireless Propagation Letters

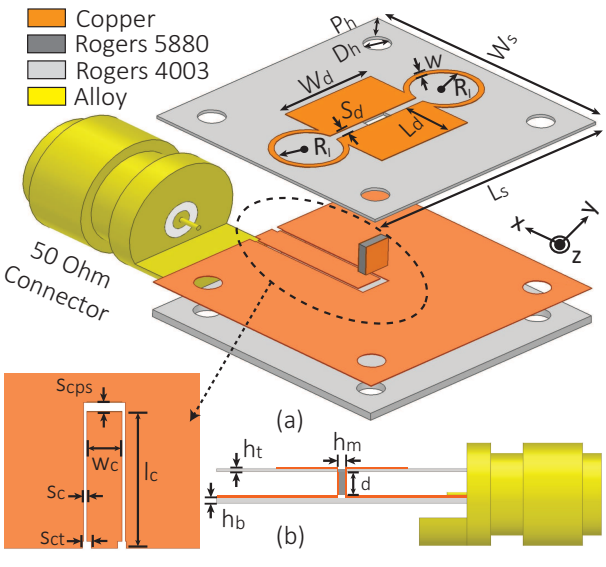

var.	L_s	W_s	L_d	W_d	S_d	R_l	w	D_h	P_h	d
val. (mm)	16	16	3.3	6.2	0.5	2.1	0.3	1.5	2.1	1.8

var.	w_c	l_c	s_c	s_{ct}	s_{cps}	h_b	h_m	h_t	t	-
val. (mm)	1.6	8	0.15	0.4	0.5	0.5	0.5	0.2	0.035	-

Fig. 1. CPW-PS line fed loop-loaded ME dipole antenna. (a) Exploded view (b) Cross-sectional view showing PS to dipole connection.

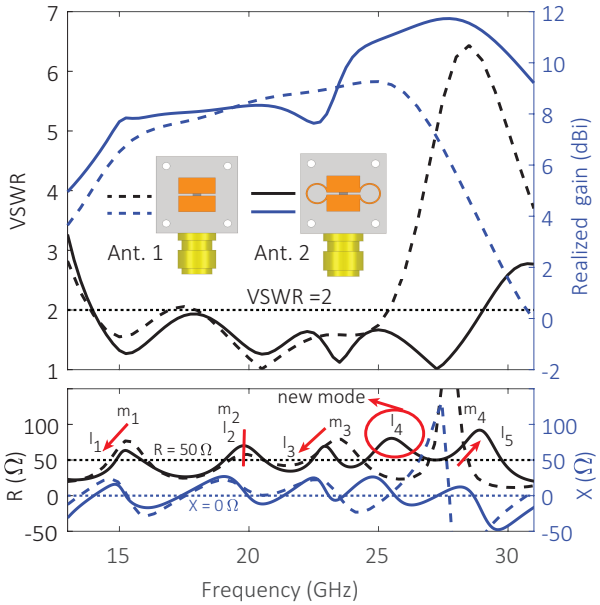

Fig. 2. Design evolution from simple MEA to LLMEA, showing antenna resonant modes in input impedances along with VSWR and realized gain. Dashed and solid lines show simple MEA and LLMEA cases respectively.

B. Simple and Loop-loaded MEAs

The top resonant structure is designed on 0.2 mm thick Rogers-4003 substrate with a slot at the center to incorporate the PS. A simple MEA (Ant. 1) shown in Fig. 2 is designed by using two metal strips of width W_d and length L_d to create two arms of the wide armed dipole. These strips are separated by a gap S_d. Thus, a W_d long slot open at both the ends is created. The top substrate is placed at an air gap of $d = 1.8$ mm as shown in Fig.1 (b) and the arms of the 50 Ω connector are removed to not interfere with top layer. The two strips of the PS line are connected to two arms of the ME dipole obtaining a balanced feed to the MEA. Furthermore, drill holes are provided in both the substrates to obtain good alignment using dowel pins. The Voltage standing wave ratio (VSWR) and the realized gain for the simple MEA case are shown in Fig. 2 with all design parameters the same as Fig.1 and W_d optimized at 7.2 mm. The antenna exhibits a fractional IBW (VSWR $\leq$ 2) of 58.76% (13.87 - 25.41 GHz) and shows 4 resonant modes m_1–m_4 as seen from the input resistance and reactance responses. These 4 resonant peaks occur at 15.30, 19.95, 23.45, and 27.76 GHz. Furthermore, the realized gain ranges from 4.91 - 9.26 dBi and drops sharply above 25.5 GHz showing ∼4.5 dB variation over the band. Notably, the IBW of this simple antenna is ∼60% which can be attributed to the broadband CPW-PS feed. Moreover, the maximum achievable realized gain is around 9 dBi.

To further improve the IBW and the gain, a simple modification is proposed. Instead of keeping the slot ends open, a metallic trace loop termination is added at both open ends, altering a simple slot into a dumbbell-shaped structure (slot ends loaded with loop). As seen in Fig. 2 (Ant. 2), the VSWR curve for the loop-loaded MEA (LLMEA) shows one more resonant mode compared to the simple MEA. If different modes of LLMEA are defined as l_1–l_5 at frequencies f_1–f_5, the new resonant mode l_4 near 25.5 GHz can be attributed to the loop termination. The simple MEA modes m_1, m_3 move slightly downwards and m_4 moves upward to become l_1, l_3, and l_5 respectively for the LLMEA case while m_2 and l_2 essentially overlap. The detailed study on modes and parametric effects are discussed in the parametric analysis in sec. III. The circumference of each loop is ∼13.2 mm and corresponds to nearly one wavelength ($1.16\lambda_g$) at 25.5 GHz (λ_g is based on effective dielectric constant [15]). Consequently, the IBW (VSWR $\leq$ 2) is enhanced and covers 13.94 - 29.05 GHz (∼70.3%). Moreover, the maximum simulated realized gain contributed by the antennas increases from 9.26 to 11.73 dBi. The realized gains after f_3 = 22.91 GHz shows a trend very similar to a 1–1.5λ long loop above the ground plane [16]. Thus, the LLMEA helps to improve both the IBW and gain, hence, will be presented in detail. Notably, the proposed antenna is simple to fabricate as it does not involve metallic vias and provides better radiation efficiency and uses lossless material (air) between the antenna and the ground plane. The simulated total efficiency of the antenna is 86-96% while the radiation efficiency is $>$ 95%.

III. Parametric Analysis

The proposed antenna shows total five magneto-electric resonant modes in the 13-31 GHz range as seen in Fig. 2. To study the dependence of these modes on design parameters, only the input resistance R of the antenna is shown. Our simulations show that the loop radius R_l, dipole width W_d, dipole length L_d are most crucial among other factors such as ground plane size and the ground spacing d. Fig. 3 shows the variation in R, VSWR, and realized gain with change in L_d, W_d, and R_l with solid line showing the curves for the optimum

This article has been accepted for publication in a future issue of this journal, but has not been fully edited. Content may change prior to final publication. Citation information: DOI 10.1109/LAWP.2021.3115234, IEEE Antennas and Wireless Propagation Letters

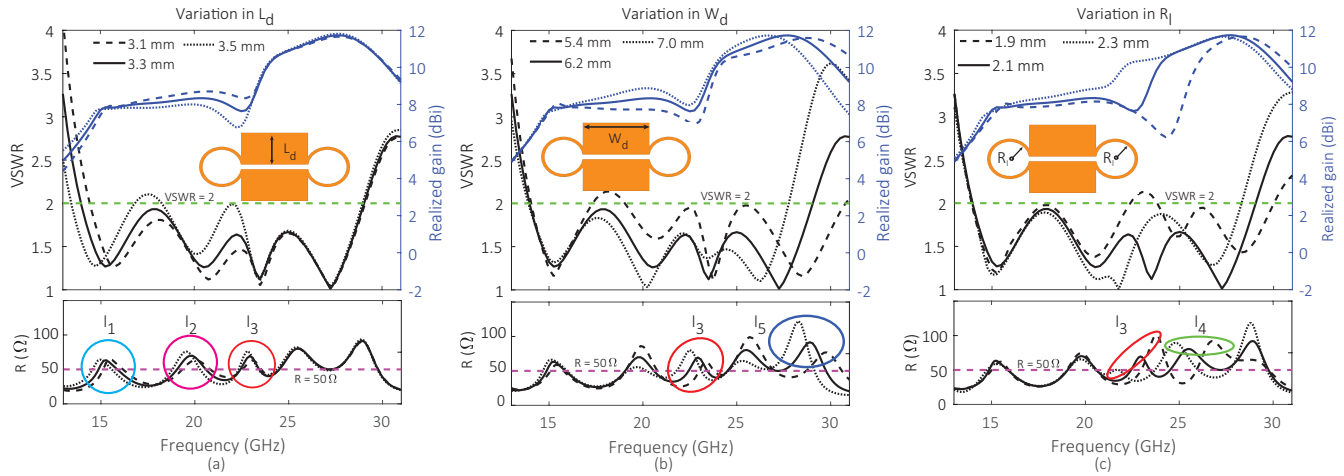

Fig. 3. Variation of VSWR, realized gain, and input resistance with change in design parameters. (a) Dipole length (L_d), (b) Dipole width (W_d), and (c) Loop Radius (R_l). Changes in each mode l_1, l_2, l_3, l_4, and l_5 are encircled in cyan, magenta, red, green, and blue colors respectively.

value. The length of the dipole L_d majorly affects modes l_1 and l_2 and shows meek effect on l_3 as seen in Fig. 3 (a). Increasing L_d shifts the affected mode downwards, improving the contributed gain and VSWR slightly near l_1 while they degrade near l_2. Notably, mode l_2 occurs at 19.91 GHz when dipole length ($L = 2L_d+S_d$) = $0.49\lambda_g$ whereas l_1 occurs at 15.54 GHz when dipole + PS length ($L+ 2d$) = $0.58\lambda_g$. Thus, these modes can be attributed to electric dipole modes. Notably, mode l_1 supported by PS line enables lower band operation while keeping the profile low. Fig. 4 (a) shows the surface current distribution (CD) at 19.91 GHz at $\omega t = 90°$ when current peaks. As seen, dipole mode dominates whereas loop currents are relatively lower.

The dipole or slot width W_d affects l_5 strongly and l_3 slightly as shown in Fig. 3 (b). The mode l_5 shifts upwards with decreasing width W_d, impedance matching near l_5 degrades although IBW and realized gain improve. Mode l_5 occurs at 28.91 GHz and the slot length is around $W_d = 0.6\lambda_g$.

Loop radius R_l shows significant impact on the modes l_3 and l_4. A downward shift is observed with larger loop circumference while l_1, l_2, and l_5 remain unchanged as seen from 3 (c). The mode l_3 occurs at 22.92 GHz, when the dipole width $W_d = 0.48\lambda_g$. However, the corresponding mode m_3 for simple MEA exists at 23.56 GHz with $W_d \sim 0.6\lambda_g$, thus, l_3 can be called loop-loaded open slot (dumbbell-shaped) mode. Fig. 4 (b) and (c) show CD near mode l_3 and l_4. The loop currents dominate near l_4 and indicates one λ_g resonance (loop circumference = $1.16\lambda_g$ at 25.54 GHz) with nulls near 90° and 270° along the loop circumference. Near mode l_3, the dipole and loops are both equally excited but oppose each other and reduce the gain near 22.50 GHz (see Fig. 2). Fig. 3 (a) – (c), indicate that the gain near l_3 depends largely upon the spacing between l_2 and l_4, it improves as they come closer. Since, there is a trade off between the IBW and gain, it is optimized to be maximum, considering gain variation over the operational bandwidth of the antenna.

Finally, the ground plane spacing d and size (L_s, W_s) play a role in impedance matching and further improve the realized gain at lower frequencies where ground size is $\sim 0.75\lambda_g$. As

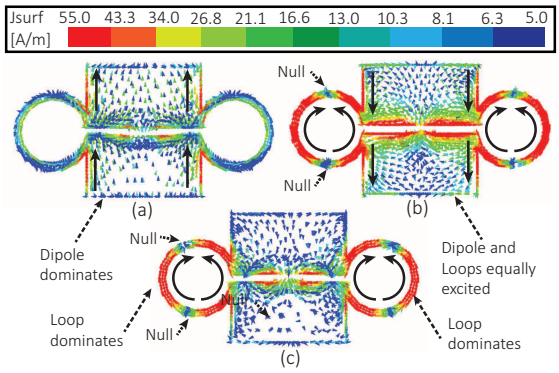

Fig. 4. Surface current distribution on the dipole loop structure at $\omega t = 90°$. (a) 19.91 GHz, (b) 22.50 GHz, (c) 25.54 GHz.

the spacing and size are changed, all the modes are affected due to change in fringing fields. The ground spacing and its size are selected as 1.8 mm and 256 mm^2 to obtain a good operating bandwidth and gain while keeping the profile low.

IV. Experimental Results

A. Antenna Prototype Fabrication

The top and bottom horizontal layers of the fabricated antenna use 0.2 mm and 0.5 mm thick Rogers 4003 substrates while the vertical PS line is housed in a 0.5 mm thick Rogers 5880. The 50 Ω CPW line is patterned on the copper cladding of the bottom substrate using in-house PCB prototyping and fed with an end-launch connector [13]. The CPW to PS line transition is realized with a 1.6 mm wide piece of Rogers 5880 substrate using the copper cladding on both the sides as the parallel plates. On the CPW side, the two plates are soldered to CPW signal trace and ground respectively while the piece length is kept longer than the required length d for easy handling. Furthermore, four drill holes are provided to aid with the alignment of substrates using dowel pins. The LLMEA is patterned on copper cladding of the top horizontal substrate and the slot is milled at the center to insert the top end of the vertical PS. The dipole strips separated by gap S_d

This article has been accepted for publication in a future issue of this journal, but has not been fully edited. Content may change prior to final publication. Citation information: DOI 10.1109/LAWP.2021.3115234, IEEE Antennas and Wireless Propagation Letters

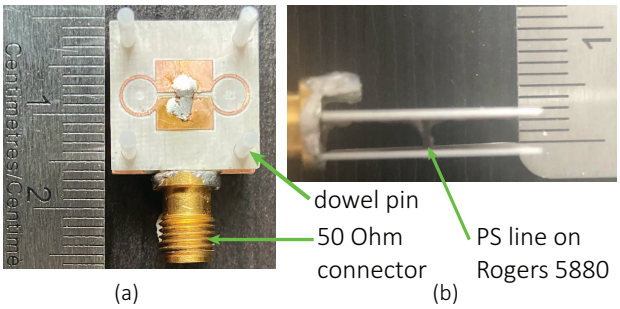

Fig. 5. Fabricated antenna prototype. (a) Top view (showing dowel pins used for alignment), (b) Cross-section view (dowel pins removed) .

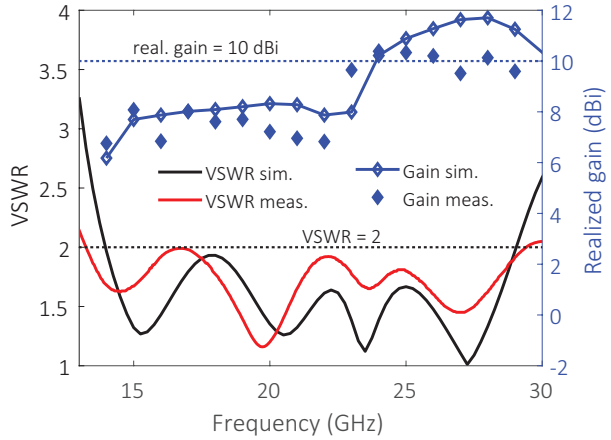

Fig. 6. Measured VSWR and realized gain for the fabricated antenna.

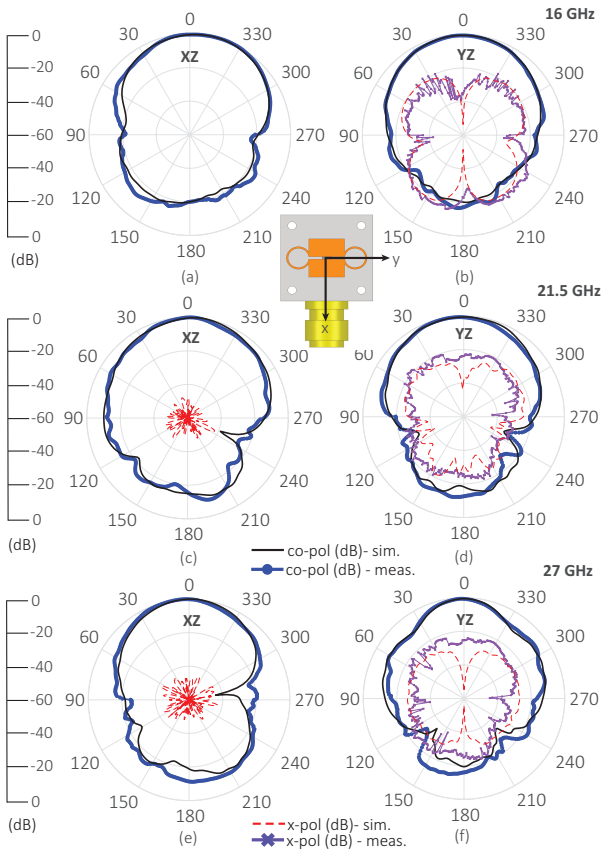

Fig. 7. Measured normalized radiation pattern of the proposed LLMEA. (a) xz-plane (16 GHz) (b) yz-plane (16 GHz) (c) xz-plane (21.5 GHz) (d) yz-plane (16 GHz), (e) xz-plane (27 GHz), (f) xz-plane (27 GHz).

are soldered to parallel plates of PS obtaining a balanced feed configuration. Lastly, the extra length of the PS is removed to obtain a flushed surface. The top and the cross-section view of the fabricated antenna are shown in Fig. 5 (a) and (b).

B. Antenna Measurements

The measured VSWR for the antenna is measured using a vector network analyzer (VNA) and shown in Fig. 6, the VSWR is ≤ 2 from 13.2 GHz to 29.3 GHz (75.76%). The measured response shows a downward shift at the lower band. The far-field response is measured inside an anechoic chamber to obtain the realized gain. As seen in Fig. 6, the measured realized gain ranges from 6.76 – 10.40 dBi (8.58$\pm$1.82 dBi from 14 to 29 GHz). Moreover, the measured gains are lower and the maxima occurs at 24 GHz.

Normalized simulated far-field radiation patterns on the xz and yz planes are shown in Fig. 7 along with measurement results. In the xz-plane, the cross-polar (x-pol) component is very low (values below -60 dB are not shown), therefore, only simulated x-pol is shown as measured values go down to noise floor of the measurement system. In the yz-plane, higher x-pol occurs towards $\pm$ 60° that could be due to PS radiation although broadside x-pol discrimination is very high with the measured x-pol $\leq$ 20 dB. The simulated and measured 3 dB beamwidth, in the xz plane are 69.2° and 69.4° at 16 GHz, 58.0° and 49.2° at 21.5 GHz, and 52.9° and 53.3° at 27 GHz respectively, whereas in the yz plane, they are 69.2° and 67.4° at 16 GHz, 63.1° and 55.3° at 21.5 GHz, and 34.8° and 36.2° at 27 GHz respectively.

CONCLUSION

A loop-loaded ME-dipole antenna (LLMEA) has been demonstrated to enhance the IBW and realized gain. Balanced feed is utilized with CPW-PS line feeding the MEA with one-point feed. The loop-loading enhances both IBW and gain by contributing an extra (λ_g) mode whereby the overall antenna size is same compared to simple MEA. It exhibits measured IBW of 75.76% with realized gain of 8.6 $\pm$ 1.8 dBi (14 to 29 GHz). Table. I provides a comparison with literature and shows that proposed element offers improved IBW and gain with a low profile and simple in-house via-less fabrication.

TABLE I
COMPARISON WITH OTHER K_u, K, AND K_a BAND ME ELEMENTS

Ref.	Feed Type	f_0 (GHz)	IBW (%)	Gain ((dBi))	Height (λ_0)	Size. (λ_0^2)
[5][a]	MSL aperture	27.75	29.1	8.3 $\pm$ 0.7	0.165	1.20[b]
[7][a]	MSL L-probe	32.15	54.4	7.35 $\pm$ 0.95	0.288	0.95
[9][a]	MSL aperture	29.08	42.78	8.2 $\pm$ 0.8[b]	0.168	-
This	CPW-PS line	21.25	75.76	8.58 $\pm$ 1.82[c]	0.177	1.28

[a] simulated element data, [b] esimate from figure [c] 14 – 29 GHz

REFERENCES

[1] A. Chlavin, "A New Antenna Feed Having Equal E -and H-plane Patterns," *Transactions of the IRE Professional Group on Antennas and Propagation*, vol. 2, no. 3, pp. 113–119, 1954.

[2] K.-M. Luk and H. Wong, "A New Wideband Unidirectional Antenna Element," *Int. J. Microw. Opt. Technol.*, vol. 1, no. 1, pp. 35–44, 2006.

[3] M. Li and K. Luk, "Wideband Magneto-Electric Dipole Antenna for 60-GHz Millimeter-Wave Communications," *IEEE Transactions on Antennas and Propagation*, vol. 63, no. 7, pp. 3276–3279, 2015.

[4] L. Cai, H. Wong, and K. Tong, "A Simple Low-Profile Coaxially-Fed Magneto-Electric Dipole Antenna Without Slot-Cavity," *IEEE Open Journal of Antennas and Propagation*, vol. 1, pp. 233–238, 2020.

[5] L. Cai and K. F. Tong, "A Millimeter-wave Aperture-coupled Simple Low-Profile Magneto-Electric Antenna," in *2020 IEEE Asia-Pacific Microwave Conference (APMC)*, 2020, pp. 1078–1080.

[6] J. Sun and K. Luk, "Wideband Magneto-Electric Dipole Antennas for Millimeter-Wave Applications with Microstrip Line Feed," in *2018 International Symp. on Antennas and Propagation (ISAP)*, 2018, pp. 1–2.

[7] J. Sun, A. Li, and K. M. Luk, "A High-Gain Millimeter-Wave Magnetoelectric Dipole Array With Packaged Microstrip Line Feed Network," *IEEE Antennas and Wireless Propagation Letters*, vol. 19, no. 10, pp. 1669–1673, 2020.

[8] Y. Li and K.-M. Luk, "60-GHz Dual-Polarized Two-Dimensional Switch-Beam Wideband Antenna Array of Aperture-Coupled Magneto-Electric Dipoles," *IEEE Transactions on Antennas and Propagation*, vol. 64, no. 2, pp. 554–563, 2016.

[9] J. Xu, W. Hong, Z. H. Jiang, and H. Zhang, "Millimeter-Wave Broadband Substrate Integrated Magneto-Electric Dipole Arrays With Corporate Low-Profile Microstrip Feeding Structures," *IEEE Transactions on Antennas and Propagation*, vol. 68, no. 10, pp. 7056–7067, 2020.

[10] M. Li and K. Luk, "A Differential-Fed Magneto-Electric Dipole Antenna for UWB Applications," *IEEE Transactions on Antennas and Propagation*, vol. 61, no. 1, pp. 92–99, 2013.

[11] F. Wu, L. Xiang, Z. Jiang, C. Yu, and W. Hong, "A Wideband Dual-Polarized Magneto-Electric Dipole Antenna for Millimeter Wave Applications," *Microwave and Optical Technology Letters*. [Online]. Available: https://onlinelibrary.wiley.com/doi/abs/10.1002/mop.32754

[12] J. Wang, Y. Li, J. Wang, L. Ge, M. Chen, Z. Zhang, and Z. Li, "A Low-Profile Vertically Polarized Magneto-Electric Monopole Antenna With a 60% Bandwidth for Millimeter-Wave Applications," *IEEE Transactions on Antennas and Propagation*, vol. 69, no. 1, pp. 3–13, 2021.

[13] SV Microwave, " Coaxial Connectors 2.92mm F Edge Launch .062 PCB Thickness," https://www.svmicrowave.com/sites/default/files/pdf/1521-60051.PDD_0.PDF, accessed: 2021-03-11.

[14] Do-Hoon Kwon and Yongjin Kim, "A Wideband Vertical Transition Between Co-Planar Waveguide and Parallel-Strip Transmission Line," *IEEE Microwave and Wireless Components Letters*, vol. 15, no. 9, pp. 591–593, 2005.

[15] I. J. Bahl, *Lumped Elements for RF and Microwave Circuits*. Norwood, MA: Artech house, 2003, ch. 5, pp. 171–172.

[16] J. L. Volakis, *Antenna Engineering Handbook*, 4th ed. New York, USA: McGraw-Hill Education, 2007, ch. 5, pp. 12 – 15.